





## Stochastic dynamics and bound states of heavy impurities in a Fermi bath

Matteo Sighinolfi <sup>1,2,\*</sup>, Davide De Boni <sup>2</sup>, Alessandro Roggero <sup>2,3</sup>, Giovanni Garberoglio <sup>4,3</sup>,  
Pietro Faccioli<sup>2,3</sup> and Alessio Recati<sup>1,2,3</sup>

<sup>1</sup>*INO-CNR BEC Center, I-38123 Trento, Italy*

<sup>2</sup>*Dipartimento di Fisica, Università di Trento, I-38123 Trento, Italy*

<sup>3</sup>*Trento Institute for Fundamental Physics and Applications, INFN, I-38123 Trento, Italy*

<sup>4</sup>*European Centre for Theoretical Studies in Nuclear Physics and Related Areas (FBK-ECT\*), I-38123 Trento, Italy*



(Received 24 November 2021; accepted 28 March 2022; published 11 April 2022)

We investigate the dynamics of heavy impurities embedded in an ultracold Fermi gas by using a generalized Langevin equation. The latter—derived by means of influence functional theory—describes how the stochastic classical dynamics of the impurities and the quantum nature of the fermionic bath manifests in the emergent interaction between the impurities and in the viscosity tensor. By focusing on the two-impurity case, we predict the existence of bound states, in different conditions of coupling and temperature, whose lifetime can be analytically estimated. Our predictions should be testable using cold-gases platforms within current technology.

DOI: [10.1103/PhysRevA.105.043308](https://doi.org/10.1103/PhysRevA.105.043308)

### I. INTRODUCTION

The concept of mediated interactions between particles due to the medium they are immersed in is ubiquitous in physics. Notable examples include the phonon-mediated interaction between electrons [1], giving rise to Bardeen-Cooper-Schrieffer superconductivity, the interaction between cluster or nuclear pasta structures mediated by the surrounding neutron fluid in the inner crust of neutron stars [2–4], and the interaction between heavy quarks mediated by a plasma of deconfined quarks and gluons, in super-hot hadronic matter [5].

Highly imbalanced mixtures of ultracold gases provide clean and tunable platforms to study medium mediated interactions. In these systems, the quasiparticles resulting from dressing impurities by the polarization of the bath are usually referred to as polarons. The study of polaron physics in cold gases was initiated by seminal experimental works on the normal-to-superfluid phase transition in imbalanced Fermi-Fermi mixtures [6,7] and the identification of the normal phase as a weakly interacting gas of polarons, in the spirit of Landau Fermi liquid theory (see, e.g., [8,9] and reference therein). Shortly after, also the case of impurities immersed in a Bose gas was experimentally realized [10,11].

Presently, the static and dynamical properties of a single polaron have been relatively well understood, at least for the case of a degenerate polarized Fermi bath, at zero temperature [12]. On the other hand, the experimental and theoretical characterization of the effect of the mediated interaction between impurities is, in general, much more challenging [13]. However, two very recent experiments have measured the effect of the mediated interaction on a Bose condensed gas in a Bose-Fermi mixture, in which the Fermi gas plays the role of the bath [14,15].

The present work aims at exploring the dynamics of heavy impurities in a Fermi bath at finite temperature, within the

framework of a generalized Langevin equation (GLE) [16] that is derived from a chain of well-controlled approximations, starting from a microscopic Feynman-Vernon influence functional [17]. In this way, we are able to provide semi-analytical expressions for both the mediated interimpurity interaction and the configuration-dependent friction tensor.

Within our approach, the effective stochastic dynamics of the heavy impurities is treated at the classical level. On the other hand, quantum effects must be fully taken into account when deriving the mediated interaction, which corresponds to a finite temperature Ruderman-Kittel-Kasuya-Yosida (RKKY) [18–20] potential, and the friction tensor.

As a case study, we analyze the dynamics of two heavy impurities. By numerically integrating their stochastic equations of motion starting from configurations in which they are close to each other, we find evidence for the formation of a transient bound state. Numerical estimates of the lifetime of this state at different temperatures agree well with the analytic calculations of the dissociation rate performed within Kramers' theory (see, e.g., Ref. [21] and references therein), thus demonstrating that the impurity pair dissociation is a thermally activated rare event.

We also find that the position-dependent off-diagonal elements in the friction tensor have important implications on the dynamics of the pair. In particular, the relative motion of two close impurities is almost frictionless, yet the presence of off-diagonal elements in the friction tensor leads to a rapid dissipation of the relative orbital angular momentum [see Fig. 3(b)].

The paper is organized as follows: In Sec. II, we derive the Feynman-Vernon influence functional for our system; in Sec. III, we describe the quantum mediated interaction and friction and derive the GLE for the dynamics of the impurities, focusing on the one- and two-impurity cases; in Sec. IV, we discuss the numerical results obtained for the dynamics of two impurities which are initially close to each other. A summary of our findings is the content of Sec. V.

\*matteo.sighinolfi@unitn.it

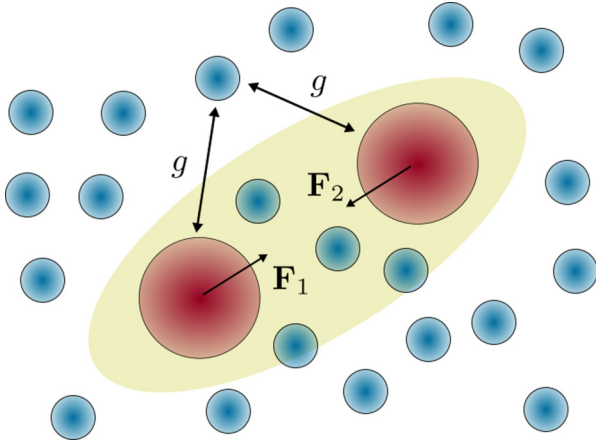


FIG. 1. Two heavy impurities (red) in a bath of fermions (cyan). The bare impurity-bath interaction  $g$  is responsible for the induced forces between impurities  $\mathbf{F}_{1,2}$  and for the low friction region (yellow).

## II. THEORETICAL SETUP

We consider a system composed by a bath of degenerate ultracold Fermi atoms of mass  $m$  and chemical potential  $\mu$ , interacting with  $N$  impurities of mass  $m_1 \gg m$ . At the energy scales we consider, particles interact only via  $s$ -wave scattering and therefore the interaction between the atoms of the bath can be neglected. For the sake of clarity, we also consider that there is no direct interaction between the impurities. The interaction between the bath and the impurities is characterized in the following by a contact potential with strength  $g$ . We also assume that the system is at a temperature  $T$  such that the de Broglie thermal wavelength of the impurities  $\lambda \sim \hbar\sqrt{2\pi/m_1 k_B T}$  is small compared to their typical interparticle distance. This will allow us to regard impurities as quasiclassical particles. In order to obtain a stochastic equation of motion for the impurities, it is convenient to describe them in first quantization and coordinate representation. We rely on quantum field theory to describe the dynamics of the degenerate fermionic bath. Our system, depicted in Fig. 1, can be modeled by the following Hamiltonian:

$$\hat{H} = \hat{H}_F + \hat{H}_I + \hat{V}, \quad (1)$$

where

$$\hat{H}_I = \sum_{i=1}^N \frac{\hat{\mathbf{p}}_i^2}{2m_1}, \quad (2)$$

$$\hat{H}_F = \int d\mathbf{x} \hat{\Psi}^\dagger(\mathbf{x}) \left( \frac{-\hbar^2}{2m} \hat{\nabla}^2 - \mu \right) \hat{\Psi}(\mathbf{x}), \quad (3)$$

$$\hat{V} = g \sum_{i=1}^N \int d\mathbf{x} \hat{\Psi}^\dagger(\mathbf{x}) \delta(\hat{\mathbf{q}}_i - \mathbf{x}) \hat{\Psi}(\mathbf{x}), \quad (4)$$

where  $\hat{\mathbf{p}}_i$  and  $\hat{\mathbf{q}}_i$  denote the impurity momentum and position operators, and  $\hat{\Psi}(\mathbf{x})$  and  $\hat{\Psi}^\dagger(\mathbf{x})$  are the annihilation and creation field operators for the particles in the bath.

Let us consider a setup in which the impurities are initially decoupled from the bath and localized at fixed positions  $\mathbf{Q}_i \equiv (\mathbf{q}_1, \dots, \mathbf{q}_N)$ . At time  $t = 0$ , the interaction with the bath is switched on and the system's density matrix begins to evolve according to the Hamiltonian (1). We are interested

in the diagonal elements of the reduced density matrix for the impurities, i.e., in the probability of observing the impurities at  $\mathbf{Q}_f = (\mathbf{q}_1^f, \dots, \mathbf{q}_N^f)$  at time  $t_f$ . Using Feynman-Vernon path integral representation of the density matrix [17] we obtain

$$P(\mathbf{Q}_f, t | \mathbf{Q}_i, 0) = \int_{\mathbf{Q}_i}^{\mathbf{Q}_f} \mathcal{D}\mathbf{Q} \int \mathcal{D}\xi \int \mathcal{D}\xi^* e^{iS[\mathbf{Q}, \xi, \xi^*]}. \quad (5)$$

In this equation,  $\xi(t, \mathbf{x})$  and  $\xi^*(t, \mathbf{x})$  are Grassmann coherent field variables, while the functional at the exponent is

$$S[\mathbf{Q}, \xi, \xi^*] = \int_{\mathcal{C}} dt' \left\{ \frac{m_1}{2} \sum_{j=1}^N \dot{\mathbf{q}}_j^2(t') + \int d\mathbf{x} \xi^*(t', \mathbf{x}) \times \left( i\hbar\partial_{t'} - \frac{\hbar^2 \nabla^2}{2m} - \mu + \rho(t', \mathbf{x}) \right) \xi(t', \mathbf{x}) \right\}, \quad (6)$$

where  $\rho(t, \mathbf{x}) = g \sum_{i=1}^N \delta(\mathbf{q}_i(t) - \mathbf{x})$  is the instantaneous impurity density and the time integral is defined over the standard Keldysh contour  $\mathcal{C}$  [22,23].

The integral over the Grassmann fields  $\xi, \xi^*$  can be carried out analytically, leading to

$$P(\mathbf{Q}_f, t | \mathbf{Q}_i, 0) = \int_{\mathbf{Q}_i}^{\mathbf{Q}_f} \mathcal{D}\mathbf{Q} e^{i\Phi_{\mathcal{C}}[\mathbf{Q}]} e^{i\frac{m_1}{2\hbar} \sum_{j=1}^N \int_{\mathcal{C}} dt' \dot{\mathbf{q}}_j^2}, \quad (7)$$

where  $\Phi_{\mathcal{C}}[\mathbf{Q}]$  is the influence functional, which is formally written as

$$i\Phi_{\mathcal{C}}[\mathbf{Q}] = \text{Tr} \left[ \ln \left( i\hbar\partial_{t'} - \frac{\hbar^2 \nabla^2}{2m} - \mu + \rho(t', \mathbf{x}) \right) \right]. \quad (8)$$

To obtain an explicit representation for  $\Phi_{\mathcal{C}}[\mathbf{Q}]$ , it is convenient to deal separately with the upper and lower branches of the Keldysh contour. In addition, we assume a low impurity density and perform a functional expansion to second order in  $\rho(t', \mathbf{x})$ . The zeroth-order term is a constant that is reabsorbed in the definition of probability, while the first-order term is an energy shift that does not affect the dynamics. The resulting expression for the transition probability density is

$$P(\mathbf{Q}_f, t | \mathbf{Q}_i, 0) = \int_{\mathbf{Q}_i}^{\mathbf{Q}_f} \mathcal{D}\mathbf{Q}' \int_{\mathbf{Q}_i}^{\mathbf{Q}_f} \mathcal{D}\mathbf{Q}'' \times e^{i\Phi(\mathbf{Q}', \mathbf{Q}'')} e^{i\frac{m_1}{2\hbar} \sum_{j=1}^N \int_0^t dt' (\dot{\mathbf{q}}_j^2 - \dot{\mathbf{q}}_j''^2)}, \quad (9)$$

where

$$\Phi(\mathbf{Q}', \mathbf{Q}'') = \frac{i}{2} \sum_{a,b=1}^2 \int_0^t dt' \int_0^t dt'' \int d\mathbf{x} \int d\mathbf{y} \times \rho_a(t', \mathbf{x}) \Delta_{ab}(t' - t'', \mathbf{x} - \mathbf{y}) \rho_b(t'', \mathbf{y}), \quad (10)$$

where  $a, b$  label the branches of the Keldysh contour  $\mathcal{C}$ , primed variables lie on the forward branch of the contour, and double-primed variables lie on the backward branch. In particular in Eq. (10),

$$\begin{aligned} \rho_1(t, \mathbf{x}) &= g \sum_i \delta(\mathbf{q}_i'(t) - \mathbf{x}), \\ \rho_2(t, \mathbf{x}) &= g \sum_i \delta(\mathbf{q}_i''(t) - \mathbf{x}), \end{aligned} \quad (11)$$

and  $\Delta_{ab}$  are the entries of a  $2 \times 2$  matrix of Green's functions:

$$\begin{aligned}\Delta_{11}(t, \mathbf{x}) &= \Delta_F(t, \mathbf{x}) = iD_F(t, \mathbf{x}), \\ \Delta_{12}(t, \mathbf{x}) &= -\Delta_{<}(t, \mathbf{x}) = -iD_{<}(t, \mathbf{x}), \\ \Delta_{21}(t, \mathbf{x}) &= -\Delta_{>}(t, \mathbf{x}) = -iD_{>}(t, \mathbf{x}), \\ \Delta_{22}(t, \mathbf{x}) &= \Delta_{\bar{F}}(t, \mathbf{x}) = iD_{\bar{F}}(t, \mathbf{x}).\end{aligned}\quad (12)$$

Here,  $D_{>}(t, \mathbf{x})$ ,  $D_{<}(t, \mathbf{x})$ , and  $D_F(t, \mathbf{x})$  are the standard fermionic polarization propagators of many-body theory [24,25].

We emphasize that expressions (9) and (10) follow directly from Eq. (7), in the small impurity density limit.

In the next section, we shall introduce additional approximations which enable us to efficiently compute the transition probability by integrating a stochastic differential equation of motions.

### III. EFFECTIVE STOCHASTIC DYNAMICS OF HEAVY IMPURITIES

In this section, we introduce a chain of well-controlled approximations to enable the sampling of the transition probability density (7).

#### A. Small frequency expansion

Since the mass of the impurities is much greater than that of the particles in the bath, the dynamics of the former is expected to be much slower. Then, it is possible to perform a small frequency expansion of  $\Delta_{ab}$  in Eq. (12):

$$\begin{aligned}\Delta_{ab}(t, \mathbf{x}) &= \int \frac{d\omega}{2\pi} e^{-i\omega t} \left( \sum_{n=0}^{\infty} \frac{\omega^n}{n!} F_{ab}^{(n)}(\mathbf{x}) \right) \\ &= F_{ab}^{(0)}(\mathbf{x}) + i \frac{d}{dt} \delta(t) F_{ab}^{(1)}(\mathbf{x}) + \dots,\end{aligned}\quad (13)$$

where

$$F_{ab}^{(0)}(\mathbf{x} - \mathbf{y}) \equiv \Delta_{ab}(\omega = 0, \mathbf{x} - \mathbf{y}), \quad (14)$$

$$F_{ab}^{(1)}(\mathbf{x} - \mathbf{y}) \equiv \lim_{\omega \rightarrow 0} \frac{d}{d\omega} \Delta_{ab}(\omega, \mathbf{x} - \mathbf{y}), \quad (15)$$

and the dots denote higher order terms in the Taylor expansion. Substituting Eqs. (13) and (11) into Eq. (10) we obtain

$$\begin{aligned}\Phi(\mathbf{Q}', \mathbf{Q}'') &= \frac{ig^2}{2} \sum_{i,j=1}^N \int_0^t du \left\{ F_F^{(0)}(\mathbf{q}'_i - \mathbf{q}'_j) \right. \\ &\quad + F_{\bar{F}}^{(0)}(\mathbf{q}''_i - \mathbf{q}''_j) - F_{<}^{(0)}(\mathbf{q}'_i - \mathbf{q}''_j) \\ &\quad - F_{>}^{(0)}(\mathbf{q}''_i - \mathbf{q}'_j) - i\dot{\mathbf{q}}_{j1} \frac{\partial}{\partial \mathbf{q}'_j} F_{>}^{(1)}(\mathbf{q}'_i - \mathbf{q}'_j) \\ &\quad \left. - i\dot{\mathbf{q}}_{j2} \frac{\partial}{\partial \mathbf{q}''_j} F_{<}^{(1)}(\mathbf{q}'_i - \mathbf{q}''_j) \right\}.\end{aligned}\quad (16)$$

It is convenient to introduce the so-called complex potential  $\mathcal{V}(\mathbf{x} - \mathbf{y})$ :

$$i\mathcal{V}(\mathbf{x} - \mathbf{y}) \equiv F_F^{(0)}(\mathbf{x} - \mathbf{y}) = V(\mathbf{x} - \mathbf{y}) + iW(\mathbf{x} - \mathbf{y}). \quad (17)$$

In Appendix A, we show that the real and imaginary part of  $\mathcal{V}$  can be expressed in terms of the retarded polarization propagator in Fourier space:

$$V(\mathbf{x} - \mathbf{y}) = \text{Re}D^R(\omega = 0, \mathbf{x} - \mathbf{y}), \quad (18)$$

$$W(\mathbf{x} - \mathbf{y}) = \frac{2}{\beta} \lim_{\omega \rightarrow 0} \frac{1}{\omega} \text{Im}D^R(\omega, \mathbf{x} - \mathbf{y}). \quad (19)$$

We also show that for a bath of noninteracting fermions in three dimensions,

$$\begin{aligned}V(\mathbf{x} - \mathbf{y}) &= -\frac{mk_F}{4\pi^4 \hbar^2} \int dq \frac{\sin(qr)}{r} \int dk f_{\text{FD}}(k, T) k \\ &\quad \times \ln \left| \frac{k + q/2}{k - q/2} \right|,\end{aligned}\quad (20)$$

$$W(\mathbf{x} - \mathbf{y}) = -\frac{m^2}{2\pi^3 \hbar^3 \beta} \int dq f_{\text{FD}}(q/2, T) q \frac{\sin(qr)}{qr}, \quad (21)$$

where  $r = |\mathbf{x} - \mathbf{y}|$  and  $f_{\text{FD}}$  is the Fermi-Dirac distribution.

In the following, we use the rescaled imaginary potential  $W_R$  as

$$W_R(\mathbf{x} - \mathbf{y}) = \frac{\beta}{2} W(\mathbf{x} - \mathbf{y}), \quad (22)$$

for an easier understanding. Indeed, with this rescaling the term  $1/\beta$  in Eq. (21) disappears.

#### B. Classical limit

We now take the classical limit for the dynamics of the impurities. In order to implement this approximation, we first perform the change of variables:

$$\mathbf{r}_i = \frac{1}{2}(\mathbf{q}'_i + \mathbf{q}''_i) \quad \mathbf{y}_i = \mathbf{q}'_i - \mathbf{q}''_i. \quad (23)$$

After an integration by parts, the free action of the impurity takes the form,

$$\exp \left( \frac{im_I}{\hbar} \sum_{i=1}^N \int_0^t dt' \ddot{\mathbf{r}}_i(t') \cdot \mathbf{y}_i(t') \right). \quad (24)$$

We expect the dominant contribution to the path integral to come from the functional region where the time integral in the exponent is small or at most of order unity. To estimate it, we note that  $\int_0^t dt' \ddot{\mathbf{r}}_i \cdot \mathbf{y}_i \sim \sqrt{k_B T / m_I} |\mathbf{y}_i|$ , where  $\sqrt{k_B T / m_I}$  is the average thermal velocity of the impurities. Then, the stationary phase condition implies  $|\mathbf{y}_i| \lesssim \sqrt{1 / m_I k_B T}$ . In the limit of heavy impurities, fluctuations of  $\mathbf{y}_i$  become small compared to all relevant length scales, thus we can expand

the influence functional to second order in  $\mathbf{y}_i$ , leading to

$$P(\mathbf{R}_f, t | \mathbf{R}_i, 0) = \int_{\mathbf{R}_i}^{\mathbf{R}_f} \mathcal{D}\mathbf{R} \int_0^t \mathcal{D}\mathbf{Y} \exp \left\{ -\frac{i}{\hbar} \int_0^t dt' \right. \\ \left. \times \left[ \mathbf{y}_i (m_1 \ddot{\mathbf{r}}_i + \Gamma_{ij}(\mathbf{R}) \dot{\mathbf{r}}_j - \mathbf{F}_i(\mathbf{R})) \right. \right. \\ \left. \left. - \frac{1}{2} \mathbf{y}_i \frac{2}{\beta} \Gamma_{ij}(\mathbf{R}) \mathbf{y}_j \right] \right\}, \quad (25)$$

where  $\mathbf{R} = (\mathbf{r}_1, \dots, \mathbf{r}_N)^T$ ,  $\mathbf{Y} = (\mathbf{y}_1, \dots, \mathbf{y}_N)^T$ , and the sum over repeated indices  $i, j = 1, \dots, N$  is understood.  $F(\mathbf{R})$  and  $\Gamma_{ij}(\mathbf{R})$  are defined as

$$\mathbf{F}_i(\mathbf{R}) = -g^2 \sum_{j=i}^N \nabla V(\mathbf{r}_i - \mathbf{r}_j), \quad (26)$$

$$\Gamma_{ij}(\mathbf{R}) = g^2 \mathcal{H}_{W_R}(\mathbf{r}_i - \mathbf{r}_j), \quad (27)$$

where  $\mathcal{H}_{W_R}$  is the Hessian of  $W_R$ .

The Gaussian integral over  $\mathbf{Y}$  can be evaluated analytically, leading to our final path integral expression for the transition probability:

$$P(\mathbf{R}_f, t | \mathbf{R}_i, 0) = \int_{\mathbf{R}_i}^{\mathbf{R}_f} \mathcal{D}\mathbf{R} e^{-\int_0^t d\tau (m_1 \ddot{\mathbf{R}} - m_1 \Gamma(\mathbf{R}) \dot{\mathbf{R}} - \mathbf{F}(\mathbf{R}))^2}. \quad (28)$$

Here, the probability for the impurities to go from  $\mathbf{R}_i$  to  $\mathbf{R}_f$  in a time  $t$  is written as a functional integral over all possible trajectories connecting the initial and the final configuration. We note that the functional at the exponent, which determines the relative statistical weight of  $\mathbf{R}(t)$  trajectories, does not explicitly depend on  $\hbar$ . Indeed, it corresponds to an Onsager-Machlup action [26], which characterizes path integral representation of the propagator in classical Fokker-Planck dynamics.

As a consequence, as explicitly shown in Refs. [27,28], the same transition probability density of Eq. (28) can be generated by the following GLE:

$$m_1 \ddot{\mathbf{r}}_i = -\Gamma_{ij}(\mathbf{R}) \dot{\mathbf{r}}_j + \mathbf{F}_i(\mathbf{R}) + \boldsymbol{\Psi}_i(\mathbf{R}, t). \quad (29)$$

The viscosity  $\Gamma(\mathbf{R})_{ij}$  and the noise term  $\boldsymbol{\Psi}_i(\mathbf{R}, t)$  satisfy the fluctuation-dissipation relations,

$$\langle \boldsymbol{\Psi}_i(\mathbf{R}, t) \rangle = 0, \quad (30)$$

$$\langle \boldsymbol{\Psi}_i(\mathbf{R}, t) \otimes \boldsymbol{\Psi}_j(\mathbf{R}, t') \rangle = \frac{2}{\beta} \Gamma_{ij}(\mathbf{R}) \delta(t - t'). \quad (31)$$

The noise  $\boldsymbol{\Psi}_i(\mathbf{R})$  depends only the relative distances between the  $i$ th impurity and all the other impurities. To conclude this section, we note that while the dynamics of the impurities has been reduced to a classical diffusion process, the quantum nature of the bath is still effectively encoded in the structure of the viscosity and force terms, derived from Eqs. (20) and (21) [29].

### C. Dynamics of a single impurity

It is instructive to apply our formalism to the case of a single impurity. For  $N = 1$ , the GLE reduces to that of a standard Brownian particle, with constant viscosity and white

noise:

$$m_1 \ddot{\mathbf{r}} = -\gamma \dot{\mathbf{r}} + \boldsymbol{\Psi}(t), \quad (32)$$

where we defined  $\mathbf{r} = \mathbf{R} = \mathbf{r}_1$  and

$$\gamma = \Gamma_{11} = -\frac{8m^4 g^2}{3\hbar^7 \pi^3} (k_B T)^2 \text{Li}_2(-e^{\beta\mu(T)}) \quad (33)$$

is the single impurity friction constant where  $\text{Li}_2$  is the dilogarithm [30]. At finite temperature, Eqs. (32) and (33) yield the conventional Einstein's diffusion law, and the kinetic energy of the impurity thermalizes with the bath. However, if the temperature is much smaller than the bath Fermi temperature  $T_F = \varepsilon_F/k_B$ , with the usual Fermi energy  $\varepsilon_F = \hbar^2 k_F^2/2m$ , Eq. (33) can be written as

$$\gamma_{T \rightarrow 0} = \frac{4\hbar k_F^2}{3\pi} \left( \frac{m}{m_r} k_F a \right)^2 \left( 1 + \frac{T^2 \pi^2}{T_F^2 3} \right). \quad (34)$$

In this equation,  $m_r = m_1 m / (m_1 + m)$  is the reduced mass and  $g$  is expressed in terms of the more physical  $s$ -wave scattering length  $a$ ,  $g = 2\pi \hbar^2 a / m_r$ . We note that the viscosity remains finite even at zero temperature. This is possible because the impurity releases energy into the bath by inducing particle-hole excitations. The same result for the viscosity Eq. (34) can also be obtained by considering the energy dissipation of an infinite mass impurity moving in the bath (see Appendix B), as discussed in Ref. [31] for the case of interacting Bose gases. Note that in the latter case (and for any superfluid system), the viscosity vanishes for  $T \rightarrow 0$ , due to the existence of the critical Landau velocity, which provides a minimal velocity for the impurity to excite the system. Interestingly, Schecter and Kamenev applied the same formalism we adopted in the present work to compute the friction in a weakly interacting Bose gas, and found that it scales as  $\gamma_{\text{BEC}} \simeq T^7$  [32].

### D. Dynamics of two impurities

Let us now consider the case of two impurities. The corresponding GLEs read

$$m_1 \ddot{\mathbf{r}}_1 = -(\gamma \dot{\mathbf{r}}_1 + \Gamma_{12}(\mathbf{r}_1 - \mathbf{r}_2) \dot{\mathbf{r}}_2) \\ + \mathbf{F}_1(\mathbf{r}_1 - \mathbf{r}_2) + \boldsymbol{\Psi}_1(\mathbf{r}_1 - \mathbf{r}_2, t), \quad (35)$$

$$m_1 \ddot{\mathbf{r}}_2 = -(\Gamma_{21}(\mathbf{r}_1 - \mathbf{r}_2) \dot{\mathbf{r}}_1 + \gamma \dot{\mathbf{r}}_2) + \\ - \mathbf{F}_1(\mathbf{r}_1 - \mathbf{r}_2) + \boldsymbol{\Psi}_2(\mathbf{r}_1 - \mathbf{r}_2, t), \quad (36)$$

in strong analogy with the old result for heavy particles in incompressible fluids [33]. It is convenient to rewrite the previous equations in terms of the relative distance between the impurities,  $\mathbf{s} = \mathbf{r}_1 - \mathbf{r}_2$ , and the center of mass  $\mathbf{r}_{\text{CM}} = (\mathbf{r}_1 + \mathbf{r}_2)/2$ :

$$m_1 \ddot{\mathbf{s}} = -(\gamma - \Gamma_{12}(\mathbf{s})) \dot{\mathbf{s}} + 2\mathbf{F}_1(\mathbf{s}) + \eta_-(\mathbf{s}, t), \quad (37)$$

$$m_1 \ddot{\mathbf{r}}_{\text{CM}} = -(\gamma + \Gamma_{12}(\mathbf{s})) \dot{\mathbf{r}}_{\text{CM}} + \frac{1}{2} \eta_+(\mathbf{s}, t), \quad (38)$$

where  $\eta_+(\mathbf{s}, t)$  and  $\eta_-(\mathbf{s}, t)$  are two Gaussian noises,

$$\eta_{\pm}(\mathbf{s}, t) = \boldsymbol{\Psi}_1(\mathbf{s}, t) \pm \boldsymbol{\Psi}_2(\mathbf{s}, t). \quad (39)$$

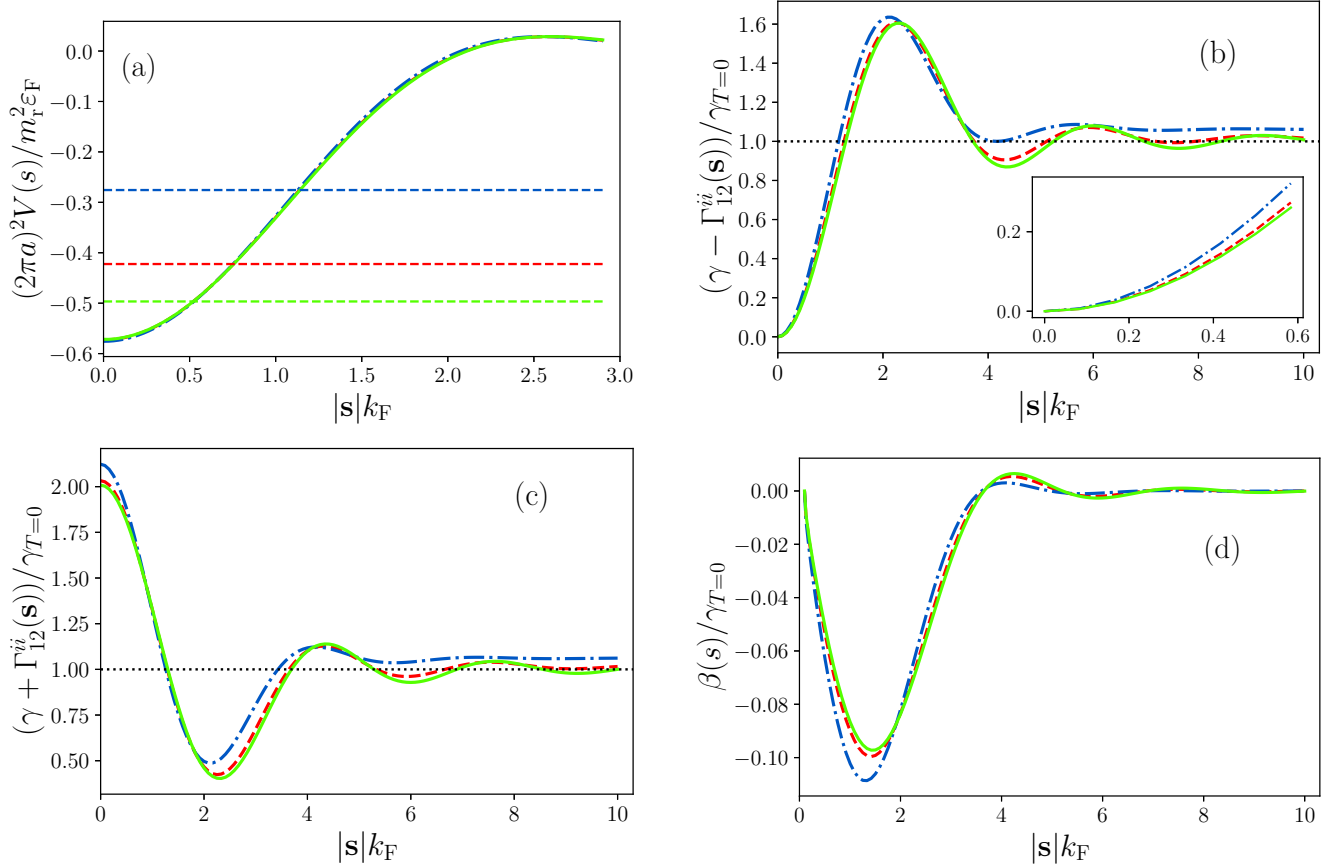


FIG. 2. Spatial dependence of the conservative potential and of the friction matrix for  $k_F a = 0.19$  and  $T/T_F = 0.2, 0.1, 0.05$  (dotted-dashed blue, dashed red, solid green lines). (a) Real potential  $V(s)$ . Horizontal dashed lines are  $V(s = 0) + 3T/2$  and their intersection with the other curves determine the typical size of the bound state  $r_b$ ; see Sec. IV for details. Note that  $V(s)$  for  $T/T_F = 0.1$  is not visible because it is hidden by the other lines. (b) Difference between the constant viscosity term and the diagonal component of the viscosity matrix  $\gamma - \Gamma_{12}^{ii}(s)$  in units of  $\gamma_{T=0}$ , i.e., Eq. (34) for  $T = 0$ . Note that  $|s|/k_F \gtrsim 6$  the oscillations decay because the contribution of  $\Gamma_{12}^{ii}$  vanishes. In the inset is shown the behavior for small  $|s|/k_F$ . (c) Sum between the constant viscosity term and the diagonal component of the viscosity matrix  $\gamma + \Gamma_{12}^{ii}(s)$  in units of  $\gamma_{T=0}$ . In the last two panels, the horizontal dotted line is a guide to the eye that mutual friction becomes irrelevant. The deviation at large distance is captured by Eq. (34). (d) Off-diagonal component strength  $\beta(s)$  of the viscosity matrix  $\Gamma_{12}^{ij}$  in units of  $\gamma_{T=0}$ . Also for the off-diagonal component the oscillatory behavior decays for  $|s|/k_F \gtrsim 6$ .

Using Eqs. (20) and (22), the explicit expression for the force and the viscosity matrix can be, respectively, written as

$$\mathbf{F}_1^i(\mathbf{s}) = \frac{mg^2}{16\pi^4 \hbar^2} \frac{s_i}{s^2} \int_0^\Lambda dq q h(q, s) \int_0^\infty dk k f_{\text{FD}}(k/2) \ln \left| \frac{k+q}{k-q} \right|, \quad (40)$$

and

$$\begin{aligned} \Gamma_{12}^{ij}(\mathbf{s}) &= \alpha(s) \delta_{ij} + \beta(s) \frac{s_i s_j}{s^2}, \\ \alpha(s) &= -\frac{m^2 g^2}{4\pi^3 \hbar^3 s^2} \int_0^\infty dq q h(q, s) f_{\text{FD}}(q/2), \\ \beta(s) &= \frac{m^2 g^2}{4\pi^3 \hbar^3 s^2} \int_0^\infty dq q (3h(q, s) + qs \sin(qs)) f_{\text{FD}}(q/2), \end{aligned} \quad (41)$$

where  $h(q, s) = \cos(qs) - \sin(qs)/(qs)$  and the function  $\beta(s)$  is the strength of the off-diagonal components of the viscosity matrix.

Note that in Eq. (40) we have introduced a UV momentum cutoff  $\Lambda$ . To be consistent with the physical interaction characterized by the  $s$ -wave scattering length  $a$ , the coupling constant must satisfy [34]

$$4k_F a = \left( \frac{\hbar^2}{2m_r} \frac{\pi}{gk_F} + \frac{\Lambda}{\pi k_F} \right)^{-1}. \quad (42)$$

The presence of a second impurity significantly modifies the stochastic equations of motion. In particular, the relative motion experiences the effect of an external force, which provides the finite temperature generalization of the RKKY interaction [18–20]. For both the center of mass and relative motion, the friction matrix is in general nondiagonal. While the diagonal components of the friction matrix possess a single-impurity and multi-impurity part, respectively, related to  $\gamma$  and  $\Gamma_{12}^{ii}$ , the off-diagonal components possess only the latter. In particular, the relative motion becomes underdamped in the limit in which the distance between the impurities is small. On the other hand, the center of mass diffuses



according to a simple Brownian motion, with a friction matrix that depends on the relative coordinate only.

The conservative potential and the friction matrix elements are plotted in Fig. 2, which also shows that the temperature dependence is very weak and that the off-diagonal component of the friction is in general much smaller than the diagonal one.

#### IV. NUMERICAL RESULTS: BOUND STATES DYNAMICS AND LIFETIME

As a case study for the dynamics of two heavy impurities in a free Fermi gas, we focus on the presence of localized (bound) solutions due to the mediated interaction and estimate their lifetime under the effect of the stochastic noise. First, we consider the typical value of the bound state size  $r_b$ : This can be estimated by matching the average kinetic energy provided by the coupling with the bath with the strength of the mediated interaction:  $(k_F a)^2 V(r_b) \propto 3k_B T/2$ . As expected, an increase in the scattering length (temperature) leads to a smaller (larger)  $r_b$ , as shown in Fig. 2(a).

We solve Eq. (29) using a stochastic Verlet algorithm [35] and simulate the time evolution of two impurities at different temperature, with scattering length  $k_F a$ . The two impurities start at rest with an initial random position  $\mathbf{s}_0$  subject to the constraint  $|\mathbf{s}_0| = r_b$ . We average over 1000 independent simulations, with a mass ratio set to  $m_1/m = 30$ , which is comparable to that of typical experimental setups (for example, in  $^{133}\text{Cs} - ^6\text{Li}$  mixtures [36] one has  $m_1/m \simeq 22$ ). With this mass ratio, the condition on the de Broglie thermal wavelength  $\lambda k_F/2\pi \ll 1$  is satisfied for all the temperatures considered, with  $2\pi/k_F$  the typical interparticle distance.

In all simulations, we find that in the long-time regime, impurities drift apart and eventually diffuse according to the single-impurity Brownian dynamics described by Eq. (32). In Fig. 3, two representative trajectories are shown: In (a) the impurities remain within a distance comparable to  $r_b$  throughout the entire simulation time shown, signaling the existence of a bound state. In (b) the impurities eventually dissociate and begin an independent Brownian diffusion.

The lifetime of the bound state  $\tau$  is defined as the average dissociation time. In the low-temperature regime (i.e., when dissociation is a thermally activated process),  $\tau$  can be calculated using Kramers' theory [21]:

$$\tau = 2\pi \sqrt{\frac{K}{K_a}} \frac{2m_1 e^{\beta U}}{\sqrt{\gamma^2 + 4Km_1} - \gamma}. \quad (43)$$

Here, the viscosity  $\gamma$  is estimated from Eq. (33) by taking the limit of vanishing distance,  $K$  and  $K_a$  are the curvature of the potential at the top and bottom of the potential energy barrier, and  $U$  is the height of the barrier.

The lifetime  $\tau$  of the bound state can also be directly inferred from the numerical simulations, indeed the bound state is considered dissociated when  $k_F s > 2.5$ , since at this interimpurity distance the slope of  $V(s)$  changes. Typical evolutions of the interimpurity distances for single trajectories are shown in Fig. 4(a) for  $k_F a = 0.19$  and  $T/T_F = 0.2$  (dotted-dashed blue line),  $T/T_F = 0.1$  (dashed red line), and  $T/T_F = 0.05$  (green line). For the latter the dissociation occurs at

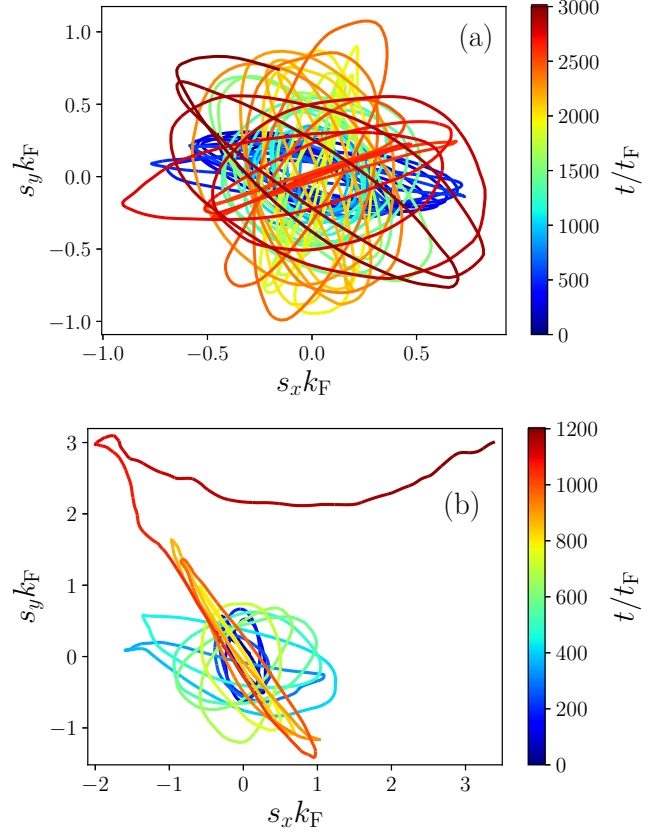


FIG. 3. Two representative trajectories obtained by integrating the GLEs starting from a configuration with relative impurity distance  $r_b$ ,  $k_F a = 0.19$ , and  $T/T_F = 0.05$ . The components  $s_x$ ,  $s_y$  of the distance  $\mathbf{s}$  are shown and the color map labels time. The motion of the impurities is also not confined on a plane due to thermal fluctuations. In the trajectory reported in (a), the impurities remain in a bound state up to  $t = 3000 t_F$ . In (b) the bound state starts to dissociate for  $t \simeq 1000 t_F$ . In this case, the relative motion in the bound state becomes quasi-one-dimensional, because of angular momentum dissipation.

$t > 350 t_F$ . We finally obtain the numerical results for the lifetime  $\tau$  by averaging over all trajectories. We observe that numerical results are in perfect agreement with the predictions of Kramers' theory Eq. (43), as shown in Fig. 4(b). This agreement implies that, at these temperatures, the dissociation of the bound states is a thermally activated event. The range of temperatures we consider is experimentally accessible. In addition, typical Fermi time  $t_F = \hbar/\varepsilon_F$  in recent experiments (see, e.g., Ref. [37]) is of order  $10^{-2}$  ms, thus dissociation times between 100 and 1000  $t_F$  should be experimentally detectable. We stress that an agreement between Kramers' theory predictions and experimental dissociation times would represent a validation of the classical approach developed in this work.

An interesting feature that can be inferred for the long-lived bound state trajectories is that the relative motion of the two impurities tends to become quasi-one-dimensional before dissociating. To analyze this feature, we study the evolution of the modulus  $L_{\text{orb}}$  of the internal orbital angular momentum  $\mathbf{L}_{\text{orb}} = \mathbf{s} \times m_1 \dot{\mathbf{s}}$ . As shown in Fig. 5 for a typical trajectory, we observe that after an initial transient time  $L_{\text{orb}}$  tends to

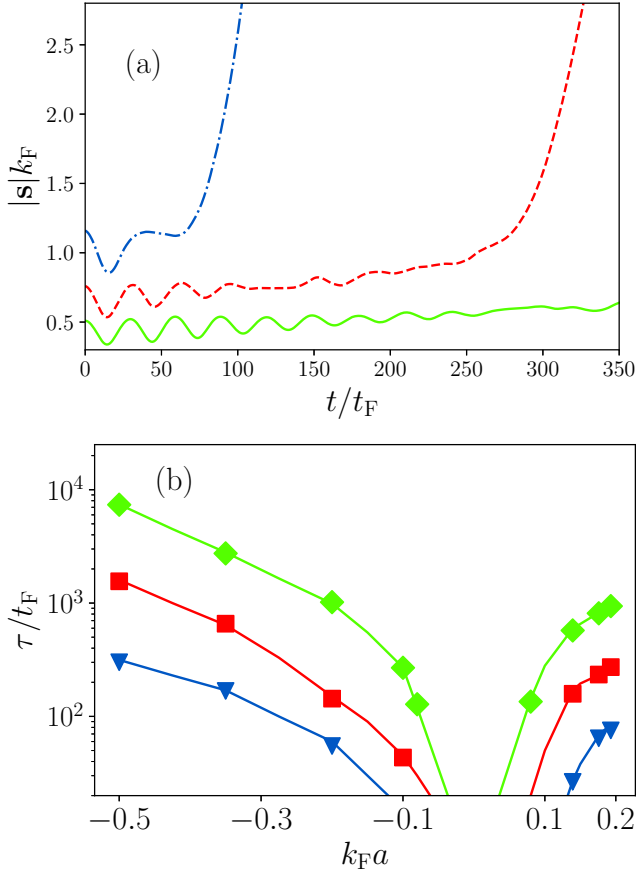


FIG. 4. (a) Single shot time evolution of  $s = |s|$  at  $k_F a = 0.19$  for different temperatures: Solid green line is  $T/T_F = 0.05$ , dashed red line is  $T/T_F = 0.1$ , and blue dotted-dashed line is  $T/T_F = 0.2$ . For  $T/T_F = 0.2$  and  $T/T_F = 0.1$ . Dissociation is visible for the higher temperatures, while it happens at longer times for  $T/T_F = 0.05$ . (b) Numerically observed lifetimes  $\tau$  as filled symbols at different  $T/T_F$  and  $k_F a$ ; lines are the theoretical predictions according to Eq. (43). Statistical uncertainties are smaller than the size of the symbols.

oscillate around a plateau value  $L_{p,s}$  and then it drops around the dissociation time. Since in the same interval the values of  $|s|$  and  $|s|$  are almost constant, the drop in internal orbital angular momentum indicates a more one-dimensional motion. The relative loss of  $L_{orb}$  for the single trajectory is calculated as  $\Delta L_s/L_{p,s} = (L_{orb}(t = \tau_s) - L_{p,s})/L_{p,s}$  and  $L_{orb}(t = \tau_s)$  is the modulus of  $L_{orb}$  at dissociation time of the single trajectory  $\tau_s$  (see Fig. 5). For a short time after dissociation we observe that  $L_{orb}$  increases rapidly due to the last momentum kick which causes the dissociation of the bound state. Finally, the average relative angular momentum loss  $\Delta L/L_p$  is calculated by averaging over all the trajectories with the same scattering length and is shown in the inset of Fig. 5.

## V. CONCLUSIONS

In a fermionic bath, the stochastic dynamics of impurities is strongly influenced by the effective interaction and friction induced by the coupling to the medium. Under a well-controlled chain of approximations, the bath degrees of

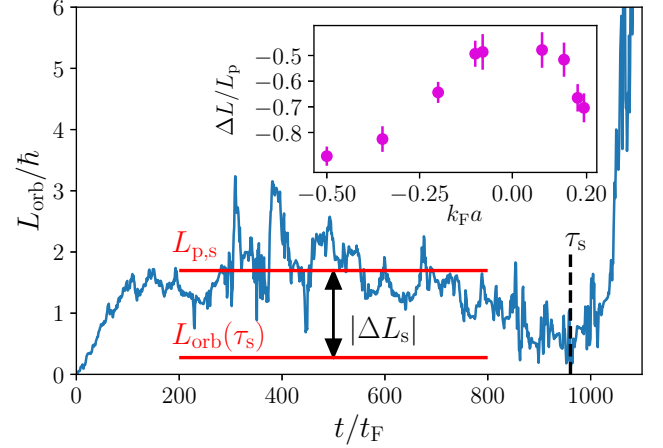


FIG. 5. Time evolution of the modulus  $L_{orb}$  of the internal orbital angular momentum with  $k_F a = 0.19$  and  $T/T_F = 0.05$  along a typical trajectory. Solid red lines indicate the plateau value  $L_{p,s}$  and the value at dissociation time  $L_{orb}(\tau_s)$ , while the vertical dashed black line indicates dissociation time  $\tau_s$ . Also the absolute value of momentum loss  $|\Delta L_s|$  is shown. (Inset) Relative momentum loss averaged over all the trajectories with the same scattering length.

freedom can be traced out and the impurities' dynamics can be described through an effective stochastic dynamics. In this scheme, the impurities obey classical GLEs, and the quantum nature of the system is encoded only in the induced force and viscosity terms.

In this work, we focused on the dynamics of a system consisting of two impurities. We found that, in the short time regime, the interplay between induced interaction and thermal fluctuations leads to the formation of a bound state characterized by a radius  $r_b$  and a lifetime  $\tau$ .

Two experimental realizations of mixtures of Bose-Einstein condensates and Fermi gas have been achieved so far [14,15]. However, the density of heavy impurities in these systems is relatively high, so that a description in terms of heavy particles independently diffusing in the medium may not be accurate. An important question to address is whether it is feasible to experimentally probe systems with lower impurity densities, using the existing technology.

Although more demanding, cold gases could also be the proper platform to obtain a direct experimental evidence of an off-diagonal component of the friction for the impurities.

We note that the same approach adopted in the present work was applied by some of us to investigate the dynamics of heavy quarks diffusing in a ultrarelativistic quark-gluon plasma [27]. That analysis was based on an effective finite temperature Abelian gauge theory to describe the dynamics in the deconfined plasma. In that approach, heavy quarks and antiquarks played the role of two distinct types of impurities, while light quarks and antiquarks formed the thermal bath. All quarks in the systems were coupled via a Debye-screened Coulomb-type interaction. As a consequence of these features, the sign of  $\Gamma_{12}$  was found to be different from that of the present Fermi system. Namely, the center-of-mass motion experiences a very reduced effective friction, while the relative internal motion of the quark-antiquark pair is overdamped. As an outlook, it could be interesting to devise a cold atom system

that can mimic such a model. This may be done by properly selecting two different hyperfine levels or two different atomic species that couple with opposite sign to the particles in the Fermi bath. The extension of the present simulation strategy to a superfluid fermionic bath and to many-body systems of impurities would also be extremely valuable to understand the properties of the outer layers of neutron stars, such as entrainment effects caused by the presence of the medium (see, e.g., [38]) and modifications to transport properties of the crust like the thermal conductivity [39,40] and the neutrino opacity [41–43].

It would also be interesting to study our results in different dimensionality, to explore the role of a longer range (RKKY-like) mediated interaction and a possibly weaker friction.

### ACKNOWLEDGMENTS

We thank J. P. Blaizot for useful discussions. Financial support from the Italian MIUR under the PRIN2017 project CEnTraL (Protocol No. 20172H2SC4), from the Provincia Autonoma di Trento, and from Q@TN, the joint laboratory between University of Trento, Fondazione Bruno Kessler (FBK), National Institute for Nuclear Physics (INFN), and National Research Council (CNR), is acknowledged.

### APPENDIX A: COMPLEX POTENTIAL

In Sec. II we introduced the matrix of polarization propagators  $\Delta_{ab}$ . Here we demonstrate that with a bath in thermal equilibrium all of these functions are related and we only need one,  $\Delta^R$ , to derive the complex potential needed for the dynamics. In position space,  $\Delta^R$  is defined as

$$\Delta^R(\mathbf{x} - \mathbf{y}) = \Delta^F(\mathbf{x} - \mathbf{y}) - \Delta^<(\mathbf{x} - \mathbf{y}). \quad (\text{A1})$$

The procedure to derive Eqs. (18) and (19) of the main text is modeled on Ref. [27]. Complex potential in the small frequency approximation is

$$\begin{aligned} i\mathcal{V}(\mathbf{q}) &= \lim_{\omega \rightarrow 0} (\Delta^R(\omega, \mathbf{q}) + \Delta^<(\omega, \mathbf{q})) \\ &= \lim_{\omega \rightarrow 0} (\text{Re}\Delta^R(\omega, \mathbf{q}) + i\text{Im}\Delta^R(\omega, \mathbf{q}) + \Delta^<(\omega, \mathbf{q})). \end{aligned} \quad (\text{A2})$$

The real part of  $\Delta^R$  is related to the spectral density  $\sigma$ . Indeed, we have  $2\text{Re}\Delta^R(\omega, \mathbf{q}) = \sigma(\omega, \mathbf{q})$ . In the small frequency approximation, therefore,

$$\text{Re}\Delta^R(\omega, \mathbf{q}) = A^R(\mathbf{q}) + \omega B^R(\mathbf{q}) + o(\omega^2). \quad (\text{A3})$$

Spectral density is odd in  $\omega$ , i.e.,  $\sigma(-\omega, \mathbf{q}) = -\sigma(\omega, \mathbf{q})$ . Therefore,  $A(q) = 0$  and

$$\text{Re}\Delta^R(\omega, \mathbf{q}) = \omega B^R(\mathbf{q}) + o(\omega^2) = \frac{1}{2}\sigma(\omega, \mathbf{q}). \quad (\text{A4})$$

Exploiting the fluctuation-dissipation relation (FDR) that is valid for a bath at equilibrium, we have

$$\Delta^< = \frac{2}{e^{\beta\omega} - 1} \text{Re}\Delta^R(\omega, \mathbf{q}). \quad (\text{A5})$$

In this last equality an algebraic relation between  $\Delta^<$  and  $\Delta^R$  is established. Thanks to this, we will be able to write  $\mathcal{V}$  only in terms of  $\Delta^R$ .

The limit  $\omega \rightarrow 0$  of Eq. (A5) is

$$\lim_{\omega \rightarrow 0} \Delta^<(\omega, \mathbf{q}) = \frac{2}{\beta} B^R(\mathbf{q}). \quad (\text{A6})$$

We now perform the limit in Eq. (A2) and we obtain

$$\mathcal{V}(\mathbf{q}) = \text{Im}\Delta^R(\omega = 0, \mathbf{q}) - i\frac{2}{\beta} B^R(\mathbf{q}). \quad (\text{A7})$$

In terms of  $D^R = -i\Delta^R$  the real and imaginary part of the complex potential now are

$$V(\mathbf{q}) = \text{Re}D^R(\omega = 0, \mathbf{q}), \quad (\text{A8})$$

$$W(\mathbf{q}) = \frac{2}{\beta} \lim_{\omega \rightarrow 0} \frac{\text{Im}D^R(\omega, \mathbf{q})}{\omega}. \quad (\text{A9})$$

In three dimensions, the full expressions of  $\text{Re}D^R$  and  $\text{Im}D^R$  in momentum space are

$$\begin{aligned} \text{Re}D(\omega, \mathbf{q}) &= -\frac{m}{2\pi^2\hbar^2} \int dk f_{\text{FD}}(k, T) \frac{k}{2q} \\ &\quad \times \left( \ln \left| \frac{k/k_{\text{F}} - v_-}{k/k_{\text{F}} + v_-} \right| - \ln \left| \frac{k/k_{\text{F}} - v_+}{k/k_{\text{F}} + v_+} \right| \right), \end{aligned} \quad (\text{A10})$$

$$\text{Im}D(\omega, \mathbf{q}) = -\frac{mk_{\text{F}}}{2\pi\hbar^2} \left[ \frac{\omega}{v_{\text{F}}q} + \frac{1}{\beta v_{\text{F}}q} \ln \left( \frac{1 + e^{\beta(v_-^2\varepsilon_{\text{F}} - \mu)}}{1 + e^{\beta(v_+^2\varepsilon_{\text{F}} - \mu)}} \right) \right], \quad (\text{A11})$$

where  $\beta = 1/k_{\text{B}}T$ ,  $v_{\pm} = \omega/qv_{\text{F}} \pm q/2k_{\text{F}}$ , and  $v_{\text{F}} = k_{\text{F}}/m$ .

### APPENDIX B: ZERO-TEMPERATURE FRICTION

As shown in Ref. [31], friction can be understood also in terms of energy dissipated by an impurity moving at velocity  $V$ ,  $\dot{E} = -F_V V$ , with  $F_V$  the velocity-dependent drag force. Following the convention of Ref. [44], Sec. 7, the energy dissipated per unit time and particle when a contact interaction of strength  $g$  is considered is

$$\begin{aligned} \dot{E} &= -\int_{-\infty}^{\infty} \frac{d\mathbf{k}}{(2\pi)^3} \int_{-\infty}^{\infty} \frac{d\omega}{2\pi} 2\pi S(\omega, \mathbf{k}) \frac{n}{2N} \omega 2\pi g^2 \delta(\omega - k_z V) \\ &= -\frac{ng^2}{2N} \frac{1}{(2\pi)^2} \int_{-\infty}^{\infty} d\mathbf{k} S(k_z V, k) k_z V = -F_V V. \end{aligned} \quad (\text{B1})$$

Now we focus on the drag force  $F_V$ :

$$\begin{aligned} F_V &= \frac{ng^2}{8N\pi^2} \int_{-\infty}^{\infty} d\mathbf{k} S(k_z V, \mathbf{k}) k_z \\ &= \frac{ng^2}{4N\pi} \iint_{-\infty}^{\infty} dk_{\perp} dk_z k_{\perp} k_z S(k_z V, \sqrt{k_z^2 + k_{\perp}^2}). \end{aligned} \quad (\text{B2})$$

In order to perform the integration in Eq. (B2), we use the expression of the dynamical structure factor  $S(k_z V, \sqrt{k_z^2 + k_{\perp}^2})$  given in Ref. [45], Sec. 2. This expression is

$$S(\omega, \mathbf{k}) = \frac{v(0)}{2} \frac{\omega}{kv_{\text{F}}} \quad \text{if} \quad 0 \leq \omega \leq kv_{\text{F}} - \frac{k^2}{2m}, \quad (\text{B3})$$

which in the small velocity limit gives the conditions  $0 \leq k_z \leq 2mv_{\text{F}}$  and  $0 \leq k_{\perp} \leq \sqrt{(2mv_{\text{F}})^2 - k_z^2}$ . Performing the



integration we obtain

$$\begin{aligned} \frac{v(0)V}{2v_F} \int_0^{2mv_F} dk_z k_z^2 \int_0^{\sqrt{(2mv_F)^2 - k_z^2}} dk_\perp \frac{k_\perp}{\sqrt{k_z^2 + k_\perp^2}} \\ = \frac{8}{3} v(0) m V k_F^3. \end{aligned} \quad (\text{B4})$$

Finally, for  $F_V$  we obtain

$$\begin{aligned} F_V &= \frac{ng^2}{4N\pi} \frac{8}{3} v(0) m V k_F^3 = \frac{3mN}{k_F^2} \frac{k_F^3}{6\pi^2} \frac{g^2}{N\pi} \frac{2}{3} m k_F^3 V \\ &= \frac{m^2 k_F^4}{3\pi^3} g^2 V = \frac{4k_F^2}{3\pi} \left( k_F a \frac{m}{m_r} \right)^2 V = \gamma_{T=0} V. \end{aligned} \quad (\text{B5})$$

In this derivation, we used  $v(0) = 3mN/k_F^2$  (see [45]) and  $n = k_F^3/6\pi^2$ . Now, comparing Eqs. (B5) and (34) we see that we recovered the same result for the friction coefficient at  $T = 0$  (the missing  $\hbar$  factor is due to the fact that in this Appendix we set  $\hbar = 1$ ).

This connection between the statistical structure factor  $S(\omega, \mathbf{k})$  gives also a useful insight on why  $\gamma$  vanishes for a Bose gas or generally for a phononic spectrum at  $T = 0$ . The dynamical structure factor in the presence of the single low-energy phonon mode reads  $S(\omega, \mathbf{q}) = S_{\mathbf{k}} \delta(\omega - c|\mathbf{k}|)$ , where  $c$  is the speed of sound. Therefore, the drag force vanishes for any impurity speed  $V < c$  (obviously in agreement with the Landau criterion for superfluidity).

On the other hand, having the fermions a continuum of particle-hole excitations at low energy, a moving object will release energy to the bath at whatever speed  $V$  it moves.

- 
- [1] G. D. Mahan, *Many-Particle Physics* (Plenum Press, New York, 1993).
- [2] A. Bulgac and P. Magierski, *Nucl. Phys. A* **683**, 695 (2001).
- [3] A. Bulgac and A. Wirzba, *Phys. Rev. Lett.* **87**, 120404 (2001).
- [4] P. Magierski, A. Bulgac, and P.-H. Heenen, *Int. J. Mod. Phys. A* **17**, 1059 (2002).
- [5] A. Rothkopf, *Phys. Rep.* **858**, 1 (2020).
- [6] Y. Shin, M. W. Zwierlein, C. H. Schunck, A. Schirotzek, and W. Ketterle, *Phys. Rev. Lett.* **97**, 030401 (2006).
- [7] G. B. Partridge, W. Li, R. I. Kamar, Y.-a. Liao, and R. G. Hulet, *Science* **311**, 503 (2006).
- [8] Y.-i. Shin, C. H. Schunck, A. Schirotzek, and W. Ketterle, *Nature (London)* **451**, 689 (2008).
- [9] A. Recati, C. Lobo, and S. Stringari, *Phys. Rev. A* **78**, 023633 (2008).
- [10] M.-G. Hu, M. J. Van de Graaff, D. Kedar, J. P. Corson, E. A. Cornell, and D. S. Jin, *Phys. Rev. Lett.* **117**, 055301 (2016).
- [11] N. B. Jørgensen, L. Wacker, K. T. Skalmstang, M. M. Parish, J. Levinsen, R. S. Christensen, G. M. Bruun, and J. J. Arlt, *Phys. Rev. Lett.* **117**, 055302 (2016).
- [12] P. Massignan, M. Zaccanti, and G. M. Bruun, *Rep. Prog. Phys.* **77**, 034401 (2014).
- [13] A. Camacho-Guardian, L. A. Peña Ardila, T. Pohl, and G. M. Bruun, *Phys. Rev. Lett.* **121**, 013401 (2018).
- [14] B. J. DeSalvo, K. Patel, G. Cai, and C. Chin, *Nature (London)* **568**, 61 (2019).
- [15] H. Edri, B. Raz, N. Matzliah, N. Davidson, and R. Ozeri, *Phys. Rev. Lett.* **124**, 163401 (2020).
- [16] A. Lampo, S. H. Lim, M. Á. García-March, and M. Lewenstein, *Quantum* **1**, 30 (2017).
- [17] R. P. Feynman and F. L. Vernon Jr., *Ann. Phys.* **281**, 547 (2000).
- [18] M. A. Ruderman and C. Kittel, *Phys. Rev.* **96**, 99 (1954).
- [19] T. Kasuya, *Prog. Theor. Phys.* **16**, 45 (1956).
- [20] K. Yosida, *Phys. Rev.* **106**, 893 (1957).
- [21] P. Hänggi, P. Talkner, and M. Borkovec, *Rev. Mod. Phys.* **62**, 251 (1990).
- [22] A. Kamenev, *Field Theory of Non-equilibrium Systems* (Cambridge University Press, Cambridge, 2011).
- [23] E. A. Calzetta and B.-L. B. Hu, *Nonequilibrium Quantum Field Theory* (Cambridge University Press, 2008).
- [24] A. L. Fetter and J. D. Walecka, *Quantum Theory of Many-particle Systems* (Courier Corporation, North Chelmsford, 2012).
- [25] G. Giuliani and G. Vignale, *Quantum Theory of the Electron Liquid* (Cambridge University Press, Cambridge, 2005).
- [26] L. Onsager and S. Machlup, *Phys. Rev.* **91**, 1505 (1953).
- [27] J.-P. Blaizot, D. De Boni, P. Faccioli, and G. Garberoglio, *Nucl. Phys. A* **946**, 49 (2016).
- [28] A. W. C. Lau and T. C. Lubensky, *Phys. Rev. E* **76**, 011123 (2007).
- [29] Within our approximations, the impurity mass  $m_i$  is not renormalized. However, this effect can be considered performing the small frequency expansion at order  $\omega^2$ , where terms proportional to  $\ddot{\mathbf{r}}_i$  and to  $\dot{\mathbf{r}}_i^2$  are present. Moreover, in the limit of  $m_i \gg m$  and in the range of interaction considered it is known to be small; see, e.g., Ref. [46].
- [30] I. S. Gradshteyn and I. M. Ryzhik, *Table of Integrals, Series, and Products* (Academic Press, Cambridge, 2014).
- [31] G. E. Astrakharchik and L. P. Pitaevskii, *Phys. Rev. A* **70**, 013608 (2004).
- [32] M. Schechter and A. Kamenev, *Phys. Rev. Lett.* **112**, 155301 (2014).
- [33] J. M. Deutch and I. Oppenheim, *J. Chem. Phys.* **54**, 3547 (1971).
- [34] C. J. Pethick and H. Smith, *Bose-Einstein Condensation in Dilute Gases* (Cambridge University Press, Cambridge, 2008).
- [35] A. Ladd, Lectures at the 3rd Warsaw School of Statistical Physics, Kazimierz, Poland (2009), <http://citeseerx.ist.psu.edu/viewdoc/download?doi=10.1.1.700.7362&rep=rep1&type=pdf>.
- [36] S. Häfner, J. Ulmanis, E. D. Kuhnle, Y. Wang, C. H. Greene, and M. Weidemüller, *Phys. Rev. A* **95**, 062708 (2017).
- [37] F. Scazza, G. Valtolina, P. Massignan, A. Recati, A. Amico, A. Burchianti, C. Fort, M. Inguscio, M. Zaccanti, and G. Roati, *Phys. Rev. Lett.* **118**, 083602 (2017).
- [38] N. Chamel, *Nucl. Phys. A* **747**, 109 (2005).
- [39] C. J. Horowitz, O. L. Caballero, and D. K. Berry, *Phys. Rev. E* **79**, 026103 (2009).
- [40] A. Roggero and S. Reddy, *Phys. Rev. C* **94**, 015803 (2016).

- [41] C. J. Horowitz, M. A. Pérez-García, J. Carriere, D. K. Berry, and J. Piekarewicz, *Phys. Rev. C* **70**, 065806 (2004).
- [42] C. J. Horowitz, D. K. Berry, M. E. Caplan, T. Fischer, Z. Lin, W. G. Newton, E. O'Connor, and L. F. Roberts, [arXiv:1611.10226](https://arxiv.org/abs/1611.10226).
- [43] A. Roggero, J. Margueron, L. F. Roberts, and S. Reddy, *Phys. Rev. C* **97**, 045804 (2018).
- [44] L. Pitaevskii and S. Stringari, *Bose-Einstein Condensation and Superfluidity* (Oxford University Press, Oxford, 2016), Vol. 164.
- [45] P. Nozières and D. Pines, *The Theory of Quantum Liquids: Superfluid Bose Liquids* (CRC Press, Boca Raton, 2018).
- [46] R. Combescot, A. Recati, C. Lobo, and F. Chevy, *Phys. Rev. Lett.* **98**, 180402 (2007).